ACS Medicinal Chemistry Letters

Letter

pubs.acs.org/acsmedchemlett

Discovery of the First Potent Inhibitors of Mutant IDH1 That Lower Tumor 2-HG *in Vivo*

Janeta Popovici-Muller,*[,†] Jeffrey O. Saunders,[‡] Francesco G. Salituro,[§] Jeremy M. Travins,[†] Shunqi Yan,[∥] Fang Zhao,[⊥] Stefan Gross,[†] Lenny Dang,[†] Katharine E. Yen,[†] Hua Yang,[†] Kimberly S. Straley,[†] Shengfang Jin,[†] Kaiko Kunii,[†] Valeria R. Fantin,[▽] Shunan Zhang,[#] Qiongqun Pan,[#] Derek Shi,[#] Scott A. Biller,[†] and Shinsan M. Su[†]

[†]Agios Pharmaceuticals, 38 Sidney Street, Cambridge, Massachusetts 02139, United States

[‡]Ember Therapeutics, 855 Boylston Street, 11th Floor, Suite B, Boston, Massachusetts 02116, United States

[§]Sage Therapeutics, 215 First Street, Cambridge, Massachusetts 02141, United States

[∥]Schrödinger, Inc., 120 West 45th Street, New York, New York 10036, United States

[⊥]Sundia MediTech Company, Ltd., Building 8, 388 Jialilue Road, Zhangjiang High-Tech Park, Shanghai 201203, China

[▽]Oncology Research Unit, Pfizer Worldwide Research and Development, La Jolla Laboratories, San Diego, California 92121, United States

[#]Shanghai ChemPartner Co., LTD, 998 Halei Road, Zhangjiang Hi-tech Park, Pudong New Area, Shanghai 201203, China

Supporting Information

ABSTRACT: Optimization of a series of R132H IDH1 inhibitors from a high throughput screen led to the first potent molecules that show robust tumor 2-HG inhibition in a xenograft model. Compound **35** shows good potency in the U87 R132H cell based assay and ~90% tumor 2-HG inhibition in the corresponding mouse xenograft model following BID dosing. The magnitude and duration of tumor 2-HG inhibition correlates with free plasma concentration.

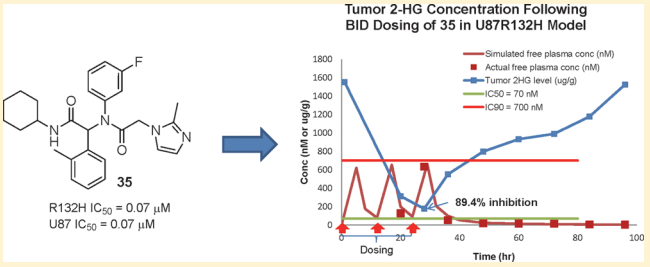

KEYWORDS: *Mutant IDH1, tumor 2-HG, R132H IDH1 inhibitors*

The family of isocitrate dehydrogenases (IDHs) includes two NADP dependent isoforms IDH1 and IDH2, which catalyze the oxidative decarboxylation of isocitrate to produce carbon dioxide, α-ketoglutarate (α-KG), and NADPH.[1,2,14]

The implication of a role for IDH in cancer was revealed after somatic mutations in IDH1 were identified through a genome wide mutation analysis in glioblastoma.[3] This landmark study was followed by high throughput sequencing, which revealed the presence of mutations in IDH1 in more than 70% of grade II–III gliomas and secondary glioblastomas,[4] as well as in approximately 10–15% of patients with acute myeloid leukemia (AML).[5] These somatic mutations were found at a key arginine residue belonging to the catalytic triad found in the enzyme's active site (R132 for IDH1). This active site mutation results in loss-of-function for the oxidative decarboxylation of isocitrate and confers a novel gain-of-function for the production of the oncometabolite D-2-hydroxyglutarate (2-HG).[6] Further characterization of the mutation showed that overexpression of mutant IDH1 in U87-MG, a human glioblastoma cell line, resulted in 100-fold elevated levels of 2-HG relative to the same cells expressing vector alone (data not shown).[6] Recently, it was demonstrated that 2-HG is a competitive inhibitor of multiple α-KG-dependent dioxygenases, including histone and DNA demethylases,[7,8] and several studies have shown that 2-HG producing IDH mutants are involved in global histone and DNA methylation alterations which may contribute to tumorigenesis through epigenetic rewiring.[9,10] Taken together, these findings implicate mutant IDH1 as an oncogene and a compelling drug target for new therapies for glioma and AML patients.

In order to identify small molecule inhibitors of IDH1,[11,12] we conducted a high-throughput screening (HTS) campaign against R132H IDH1 mutant protein homodimer. Library screen followed by confirmation of the active hits provided phenyl-glycine inhibitor **1**. Detailed kinetic mechanism-of-action studies showed compound **1** binding to be reversible and behaving as competitive inhibitor with respect to α-KG and uncompetitive with respect to NADPH (data not shown). Given its attractive chemical structure and well-defined inhibitory properties, we selected this compound as a starting point for further optimization.

Received: August 3, 2012
Accepted: September 1, 2012
Published: September 17, 2012

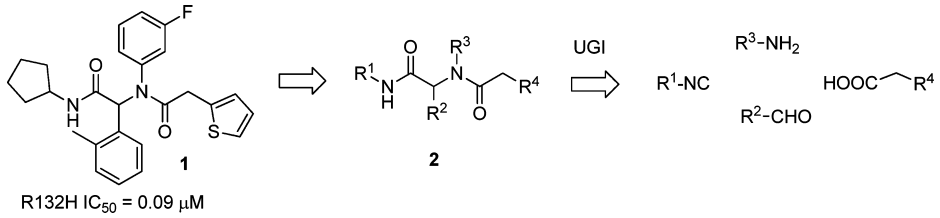

Figure 1. HTS hit **1** and phenyl-glycine scaffold synthesis.

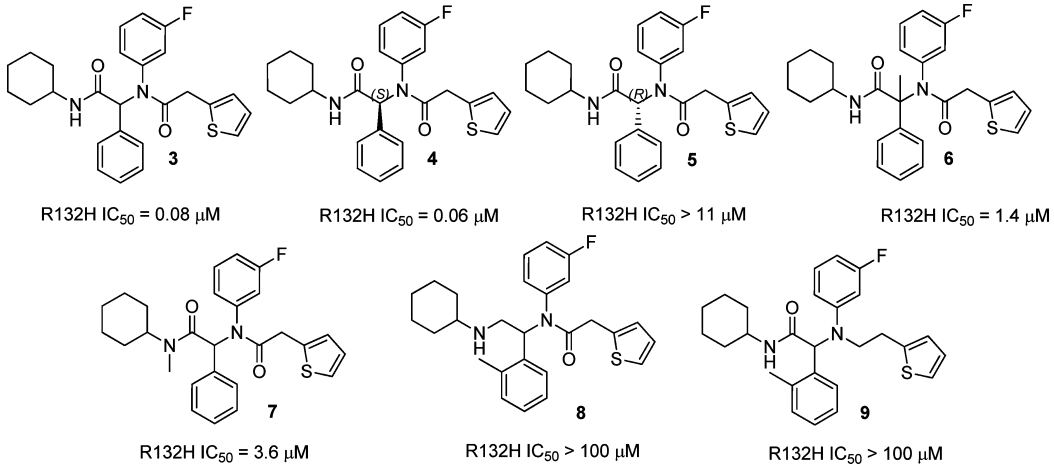

Figure 2. Key structural elements that influence the binding affinity of the phenyl-glycine scaffold.

Table 1. C-Terminus R^1 SAR

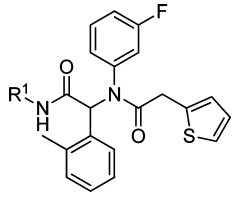

Compound	1	10	11	12	13	14	15	16	17
R^1									
clogP	5.6	6.2	5.1	5.4	4.7	5.7	6.0	3.8	3.7
R132H (μM)[a]	0.09	0.05	0.29	0.86	2.88	0.57	1.8	0.64	53.1

[a]The IC_{50} values for the R132H homodimer are the mean of at least two determinations performed as described in the Supporting Information.

We report herein that optimization of **1** led to the identification of **35**, the first reported R132H IDH1 inhibitor to show robust *in vivo* reduction of 2-HG levels in a tumor xenograft model.

The phenyl-glycine scaffold was readily assembled via four component Ugi reaction,[13] as depicted retrosynthetically in Figure 1. Compound **1** was synthesized using cyclopentyl isocyanide, *o*-methyl benzaldehyde, *m*-fluoroaniline, and (2-thiophen-2-yl) acetic acid as starting materials. If 2-chloroacetic acid is used for the Ugi acid component, intermediate **2** (R^4 = Cl) is readily obtained and can be used for further functionalization at R^4 through nucleophilic displacement of the chlorine.

Upon identification of **1** as a screening hit, we set out to understand the key structural elements that were responsible for the binding affinity of this compound to the R132H IDH1 protein (Figure 2). The molecule displays mostly hydrophobic features, with three aromatic rings positioned around two amide carbonyl groups, with a rather high clogP (5.6). Starting from a closely related analog **3** (IC_{50} = 0.08 μM), we first initiated a substitution pattern investigation of the phenyl-glycine backbone. The eutomer/distomer relationship of the α-carbon stereocenter was established by chiral synthesis of analog **3** starting from D-and L-mandelic acid,[14] which provided **4** (*S*) and **5** (*R*) enantiomers, respectively, with compound **4** (IC_{50} = 0.06 μM) possessing essentially all of the activity found in the racemate. The enantiospecificity of this enzyme inhibition held true in many analogs subsequently investigated (data not shown).

For rapid exploration of structure−activity relationships (SARs), all subsequent compounds were profiled in their racemic form. Geminal substitution at the α-carbon as depicted

dx.doi.org/10.1021/ml300225h | ACS Med. Chem. Lett. 2012, 3, 850−855

Table 2. N-Terminus R^4 SAR

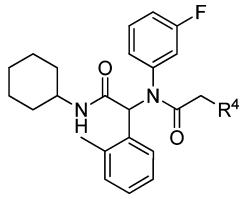

Compound	R^4	clogP	R132H (μM)[a]	Compound	R^4	clogP	R132H (μM)[a]
18	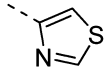	4.9	0.1	28	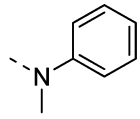	6.8	0.08
19		5.0	0.05	29	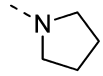	5.6	1.63
20	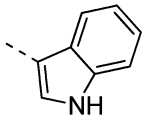	6.5	0.06	30	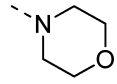	5.0	0.24
21	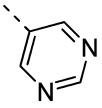	4.1	1.1	31	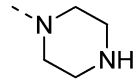	4.6	5.64
22	Cl	5.3	0.9	32	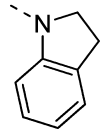	7.0	0.14
23	NH2	3.9	7.8	33	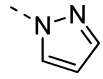	4.9	0.42
24	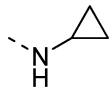	4.9	0.19	34	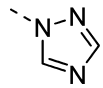	3.9	0.14
25	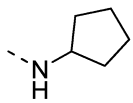	5.8	0.45	35	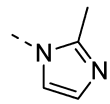	4.7	0.07
26	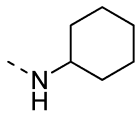	6.3	1.27	36	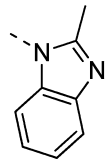	6.3	0.08
27	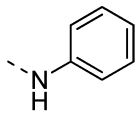	6.1	0.06	37	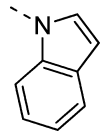	7.1	0.07

[a]The IC_{50} values for R132H homodimer are the mean of at least two determinations performed as described in the Supporting Information.

for **6** incurred an 18-fold potency loss compared to the case of **3**. Next, alkylation of the secondary amide nitrogen as shown for **7** caused a 45-fold loss in potency compared to the case of **3**, while replacement of either the C-terminus or N-terminus carbonyl groups (compounds **8** and **9**) with a CH_2 moiety resulted in significant loss of biochemical activity, highlighting the importance of both amide moieties for binding affinity.

We then started a systematic investigation of SAR for the N- and C-terminus regions of the scaffold, as well as the central aromatic moieties, with a key objective to improve properties, including decreasing the lipophilicity of the initial hit **1**, while improving biochemical potency.

R^1 functional group exploration (Table 1) revealed that carbocycles were well tolerated, with cyclohexyl **10** slightly better (IC_{50} = 0.05 μM) than the starting HTS hit **1**. As the

dx.doi.org/10.1021/ml300225h | ACS Med. Chem. Lett. 2012, 3, 850−855

Table 3. Selectivity and Cell Based Profiling of Potent Phenyl-Glycine Analogs

compd	cLogP	R132H $IC_{50}(\mu M)^a$	U87 IC_{50} (μM)	U87 GI_{50} (μM)	R132C IC_{50} (μM)^a	HT1080 IC_{50} (μM)	HT1080 GI_{50} (μM)	IDH1wt IC_{50} (μM)^b
1	5.6	0.09	0.58	>20	0.05	0.39	>20	7.7 (32%)
10	6.2	0.05	0.19	>20	0.03	0.15	>20	2.9 (22%)
18	4.9	0.10	0.29	>20	0.06	0.22	>20	19.7 (32%)
19	5.0	0.05	0.21	>20	0.05	0.26	>20	19.3 (34%)
20	6.5	0.06	0.36	>20	0.03	0.09	>3	6.3 (39%)
35	4.7	0.07	0.07	>20	0.16	0.48	>20	>100
36	6.3	0.08	0.24	>20	0.04	0.11	>20	>100
37	7.1	0.07	0.37	>20	0.04	0.17	>20	>100

^{a}The IC50 values for R132H and R132C and wt homodimers are the mean of at least two determinations performed as described in the Supporting Information. ^{b}For compounds with less than 100% enzyme inhibition, the maximum inhibition achieved is shown.

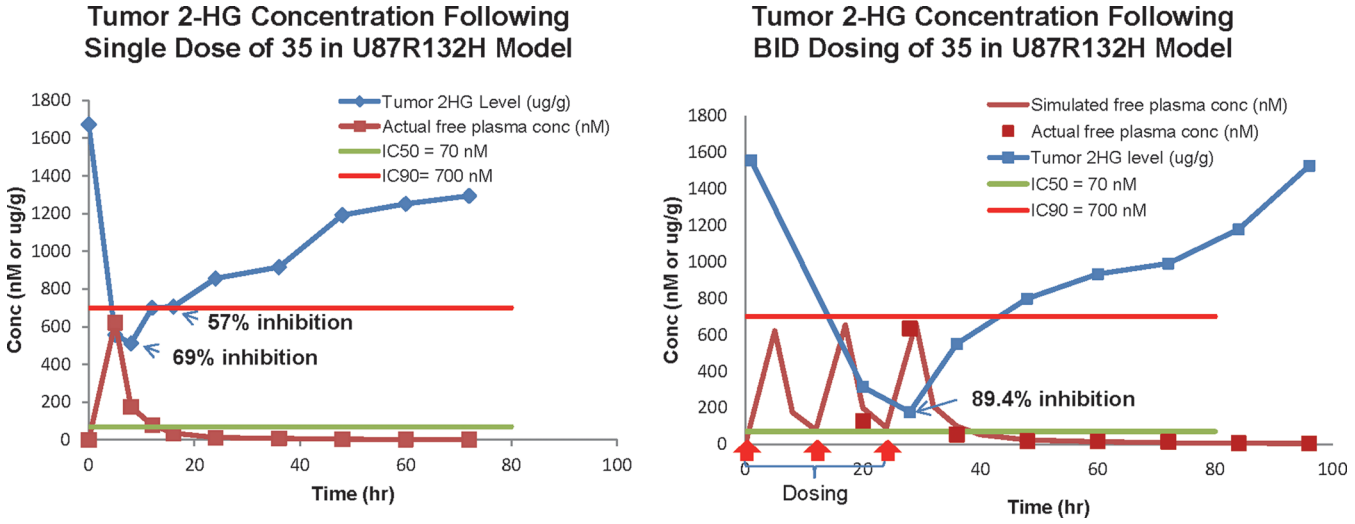

Figure 3. Tumor 2-HG inhibition following one and three BID doses of 150 mg/kg of **35** via IP route in the U87 R132H tumor xenograft model.

ring size decreased from cyclohexyl **10** to cyclopropyl **13**, potency decreased gradually to low micromolar values. Replacement of cyclohexyl with aromatic rings (*o*-tolyl, benzyl) as shown for **14** and **15** led to a 10−30-fold decrease in biochemical potency compared to the case of **10**. In an attempt to improve the properties of these compounds by decreasing the clogP through heteroatom substitution in the cyclohexyl ring, we found that pyran **16** was 10-fold less potent than **10**, while piperidine **17** suffered a nearly 100-fold loss of biochemical potency.

Evaluation of R^2 substituents revealed that for the α-aromatic ring *ortho*-substitution was most favored, while replacement of the phenyl group with heterocycles or carbocycles afforded only low micromolar potency analogs.[14] A preliminary survey of R^3 pointed to *meta*-substituted aromatic groups being most favorable, while aliphatic moieties, acyclic or cyclic, or heteroatom containing carbocycles provided analogs with a significant drop in biochemical potency.[14] These observations coupled with the C-terminus amide SAR results shown in Table 1 suggested that the phenyl-glycine scaffold was binding in a highly lipophilic region of the enzyme.

Having elucidated SAR on three areas of the scaffold, we continued our exploration on the N-terminus R^4 substituents in an additional approach to improve the compound physical chemical properties and decrease the overall lipophilicity of the original hit. Synthetic chemistry readily amenable to parallel arrays allowed us to rapidly explore a variety of functional groups at the N-terminus (Table 2).

Replacement of thiophene in compound **1** by other carbon-linked heterocycles, such as thiazole **18**, 4-pyridyl **19**, or 3-indole **20** analogs, provided similar biochemical potency to **1** in the 0.05−0.1 μM range. Modification of the pyridine **19** to pyrimidine **21** caused a 22-fold drop in potency. Our investigation next focused on nitrogen linked systems directly prepared from intermediate **2** (R^4 = Cl) via chlorine displacement (Figure 1). Replacement of chlorine in compound **22** with amino group in analog **23** caused a potency drop from 0.9 to 7.8 μM. A small set of cycloalkyl amines with an adjustment of ring size led to diminishing biochemical potency from cyclopropyl **24** (0.19 μM) to cyclohexyl **26** (1.27 μM). Interestingly, when the cyclohexyl group in **26** was replaced by a phenyl ring in compound **27**, biochemical potency was substantially enhanced from 1.27 μM to 0.06 μM. Alkylation of the aniline nitrogen as shown in analog **28** maintained the potency at 0.05 μM. Use of aromatic rings for R^4 did improve the potency compared to the aliphatic analogs (**24**−**26**); however, clogP increased as well, retaining their highly hydrophobic character. Encouraged by the good potency of aromatic tertiary amine **28**, we next tested a small set of tertiary aliphatic amines, with the aim of decreasing the lipophilicity of the scaffold by introduction of basic solubilizing groups. Among the examples that were evaluated, morpholine **30** displayed the best biochemical potency (0.24 μM), while pyrrolidine **29** and piperazine **31** afforded weakly active single digit micromolar analogs. Addition of a fused phenyl ring to pyrrolidine as shown in **32** improved the potency by 10-fold at the expense of an

dx.doi.org/10.1021/ml300225h | *ACS Med. Chem. Lett.* 2012, 3, 850−855

increased clogP value. We then continued exploration of nitrogen heterocycles from intermediate **2**. Replacing the pyrrolidine ring in compound **29** with pyrazole **33** improved biochemical potency by 4-fold, while triazole **34** offered a slight improvement in binding affinity. Gratifyingly, *N*-(2-methyl)-imidazole **35** restored the biochemical potency to 0.07 μM, while fused nitrogen linked heterocycles (benzimidazole **26**, indole **37**) maintained the same potency at the expense of increased clogP values. Overall, R^4-substitution allowed introduction of a diverse set of substituents that were well tolerated, possibly indicating that this part of the phenyl glycine scaffold may be binding in a solvent exposed area of the protein.

As the SAR investigation revealed functional group modifications that provided potent inhibitors in the R132H enzymatic assay, we selected a focused set of analogs for evaluation against R132C IDH1 mutant[15] and wild-type IDH1 enzymes. Additionally, compounds were profiled in the glioblastoma U87 cells that overexpress mutant R132H IDH1, as well as the HT1080 chondrosarcoma cell line, which expresses the endogenous R132C IDH1 mutant.[16] These cell lines produce significant levels of 2-HG compared to vector cells alone. Upon treatment with inhibitor for 48 h, the levels of 2-HG were measured in the media by LCMS, to generate IC_{50} values.[14] Within the same experiment, 50% growth inhibition (GI_{50}) was determined by measuring total cellular ATP after 72 h of compound treatment.

As shown in Table 3, the majority of compounds showed similar biochemical potency against the R132C IDH1 mutant and displayed cellular IC_{50} values less than 0.5 μM in both U87 and HT1080 cell lines, with a 3−5-fold shift in enzyme to cell potency in most cases. Exquisite selectivity for R132H and R132C IDH1 mutant isoforms was demonstrated by the poor biochemical activity against the wild-type IDH1 and the lack of induction of nonspecific cell death (GI_{50} > 20 μM).

Compound **35**, equipotent in both enzyme R132H and U87 cellular assays, was selected for additional *in vivo* profiling in the U87 R132H tumor xenograft mouse model (Figure 3). *In vitro* and *in vivo* DMPK studies were conducted for compound **35**. This analog showed rapid turnover in human and rat microsomal incubations with an estimated hepatic extraction ratio of 0.93 and 0.85, respectively. Plasma protein binding was 95.7% in mouse using the equilibrium dialysis method. Reasonable plasma exposure was achieved via intraperitoneal dosing at 50 mg/kg (AUC_{0-24h} = 20800 h·ng/mL), enabling the use of inhibitor **35** for further *in vivo* studies. Female nude mice bearing U87 R132H tumor xenografts[14] were dosed via IP route with 150 mg/kg of **35** formulated in 0.5% MC and 0.2% Tween 80, and then they were compared to the vehicle control animals. Blood and tumor samples were taken at different time points following compound administration. The plasma and tumor concentrations of inhibitor **35**, as well as the corresponding tumor 2-HG concentrations were determined using sensitive and specific LC/MS/MS methods. The unbound plasma concentration of **35** was calculated using the total plasma concentration of **35** and free fraction of **35** in mouse plasma (4.3%).

Following a single dose of **35**, the estimated plasma free concentration of **35** was higher than the *in vitro* cellular IC_{50} value (0.07 μM) for over 10 h. The magnitude and duration of tumor 2-HG inhibition correlated well with the free plasma concentration of **35**. Compared to a single dose, a repeat dose of **35** provided longer exposure coverage time (drug exposure > IC_{50}) while the C_{max} of **35** was similar following single and BID dosing. Better tumor 2-HG inhibition was achieved following BID dosing compared to a single dose, where the maximum tumor 2-HG inhibition was 89.4% and 69%, respectively. These results demonstrated that tumor 2-HG inhibition correlated with the duration of drug exposure and that robust tumor 2-HG inhibition is achievable with adequate and sustainable drug exposure.

In conclusion, we have discovered the first class of potent IDH1 mutant inhibitors through optimization of HTS hits. Compound **35** is a potent inhibitor of 2-HG production in U87 R132H cells and shows ∼90% tumor 2-HG inhibition *in vivo* following three BID doses. As high levels of 2-HG have been shown to alter the epigenetic state and biology of cells,[9,10,17] the utility of this molecule will be important to assess the biological consequences of IDH mutations and the potential of IDH inhibitors for treating IDH mutant tumors.

■ ASSOCIATED CONTENT

Supporting Information

Experimental procedures for assay protocols, *in vivo* studies, and synthesis and characterization of compounds. This material is available free of charge via the Internet at http://pubs.acs.org.

■ AUTHOR INFORMATION

Corresponding Author

*Tel: (617) 649-8604. Fax: (617) 649-8618. E-mail: janeta.popovici-muller@agios.com.

Notes

The authors declare no competing financial interest.

■ ACKNOWLEDGMENTS

We thank Dr. Nageshwara Rao KV and Dr. Sarma BVNBS at SAI Advantium for their contribution to the synthesis of compound **8**.

■ REFERENCES

(1) Yen, K. E.; Bittinger, M. A.; Su, S. M.; Fantin, V. R.; Cancer-associated, I. D. H. Mutations: biomarker and therapeutic opportunities. *Oncogene* **2010**, *29*, 6409−6417.

(2) Reitman, Z. J.; Yan, H. Isocitrate dehydrogenase 1 and 2 mutations in cancer: alterations at a crossroads of cellular metabolism. *J. Natl. Cancer Inst.* **2010**, *102*, 932−941.

(3) Parsons, D. W.; Jones, S.; Zhang, X.; Lin, J. C.; Leary, R. J.; Angenendt, P.; Mankoo, P.; Carter, H.; Siu, I. M.; Gallia, G. L.; Olivi, A.; McLendon, R.; Rasheed, B. A.; Keir, S.; Nikolskaya, T.; Nikolsky, Y.; Busam, D. A.; Tekleab, H.; Diaz, L. A., Jr.; Hartigan, J.; Smith, D. R.; Strausberg, R. L.; Marie, S. K.; Shinjo, S. M.; Yan, H.; Riggins, G. J.; Bigner, D. D.; Karchin, R.; Papadopoulos, N.; Parmigiani, G.; Vogelstein, B.; Velculescu, V. E.; Kinzler, K. W. An integrated genomic analysis of human glioblastoma multiforme. *Science* **2008**, *321*, 1807−1812.

(4) Yan, H.; Parsons, D. W.; Jin, G.; McLendon, R.; Rasheed, B. A.; Yuan, W.; Kos, I.; Batinic-Haberle, I.; Jones, S.; Riggins, G. J.; Friedman, H.; Friedman, A.; Reardon, D.; Herndon, J.; Kinzler, K. W.; Velculescu, V. E.; Vogelstein, B.; Bigner, D. D. IDH1 and IDH2 mutations in gliomas. *N. Engl. J. Med.* **2009**, *360*, 765−73.

(5) Paschka, P.; Schlenk, R. F.; Gaidzik, V. I.; Habdank, M.; Krönke, J.; Bollinger, L.; Späth, D.; Kayser, S.; Zucknick, M.; Götze, K.; Horst, H. A.; Germing, U.; Döhner, H.; Döhner, K. IDH1 and IDH2 mutations are frequent genetic alterations in acute myeloid leukemia and confer adverse prognosis in cytogenetically normal acute myeloid leukemia with NPM1 mutation without FLT3 internal tandem duplication. *J. Clin. Oncol.* **2010**, *28*, 3636−3643.

(6) Dang, L.; White, D. W.; Gross, S.; Bennett, B. D.; Bittinger, M. A.; Driggers, E. M.; Fantin, V. R.; Jang, H. G.; Jin, S.; Keenan, M. C.; Marks, K. M.; Prins, R. M.; Ward, P. S.; Yen, K. E.; Liau, L. M.; Rabinowitz, J. D.; Cantley, L. C.; Thompson, C. B.; Vander Heiden, M. G.; Su, S. M. Cancer-associated IDH1 mutations produce 2-hydroxyglutarate. *Nature* **2009**, *462*, 739−44.
(7) Xu, W.; Yang, H.; Liu, Y.; Yang, Y.; Wang, P.; Kim, S. H.; Ito, S.; Yang, C.; Wang, P.; Xiao, M. T.; Liu, L. X.; Jiang, W. Q.; Liu, J.; Zhang, J. Y.; Wang, B.; Frye, S.; Zhang, Y.; Xu, Y. H.; Lei, Q. Y.; Guan, K. L.; Zhao, S. M.; Xiong, Y. Oncometabolite 2-hydroxyglutarate is a competitive inhibitor of α-ketoglutarate-dependent dioxygenases. *Cancer Cell* **2011**, *19*, 17−30.
(8) Chowdhury, R.; Yeoh, K. K.; Tian, Y. M.; Hillringhaus, L.; Bagg, E. A.; Rose, N. R.; Leung, I. K.; Li, X. S.; Woon, E. C.; Yang, M.; McDonough, M. A.; King, O. N.; Clifton, I. J.; Klose, R. J.; Claridge, T. D.; Ratcliffe, P. J.; Schofield, C. J.; Kawamura, A. The oncometabolite 2-hydroxyglutarate inhibits histone lysine demethylases. *EMBO Rep.* **2011**, *12*, 463−469.
(9) Lu, C.; Ward, P. S.; Kapoor, G. S.; Rohle, D.; Turcan, S.; Abdel-Wahab, O.; Edwards, C. R.; Khanin, R.; Figueroa, M. E.; Melnick, A.; Wellen, K. E.; O'Rourke, D. M.; Berger, S. L.; Chan, T. A.; Levine, R. L.; Mellinghoff, I. K.; Thompson, C. B. IDH mutation impairs histone demethylation and results in a block to cell differentiation. *Nature* **2012**, *483*, 474−478.
(10) Turcan, S.; Rohle, D.; Goenka, A.; Walsh, L. A.; Fang, F.; Yilmaz, E.; Campos, C.; Fabius, A. W.; Lu, C.; Ward, P. S.; Thompson, C. B.; Kaufman, A.; Guryanova, O.; Levine, R.; Heguy, A.; Viale, A.; Morris, L. G.; Huse, J. T.; Mellinghoff, I. K.; Chan, T. A. IDH1 mutation is sufficient to establish the glioma hypermethylator phenotype. *Nature* **2012**, *483*, 474−478.
(11) Popovici-Muller, J.; Salituro, F. G.; Saunders, J. O.; Travins, J.; Yan, S. Preparation of cycloalkylheteroarylacetylphenylaminophenylacetamide derivatives and analogs for use as antitumor agents. WO 2012009678.
(12) Salituro, F. G.; Saunders, J. O. Preparation of piperazinylcarbonyl benzenesulfonamides for use in the treatment of cancer characterized as having an IDH mutation. WO 2011072174.
(13) Ugi, I.; Meyr, R.; Fetzer, U.; Steinbrückner, C. Versuche mit Isonitrilen. *Angew. Chem.* **1959**, *71* (11), 386. Ugi, I.; Lohberger, S.; Karl, R. The Passerini and Ugi Reactions, Chapter 4.6. *Comprehensive Organic Synthesis* **1991**, *2*, 1083−1109.
(14) See Supporting Information.
(15) Hartmann, C.; Meyer, J.; Balss, J.; Cappe, D.; Mueller, W.; Christians, A.; Felsberg, J.; Wolter, M.; Mawrin, C.; Wick, W.; Weller, M.; Herold-Mende, C.; Unterberg, A.; Jeuken, J. W.; Wesseling, P.; Reifenberger, G.; von Deimling, A. Type and frequency of IDH1 and IDH2 mutations are related to astrocytic and oligodendroglial differentiation and age: a study of 1,010 diffuse gliomas. *Acta Neuropathol.* **2009**, *118*, 469−474.
(16) Amary, M. F.; Bacsi, K.; Maggiani, F.; Damato, S.; Halai, D.; Berisha, F.; Pollock, R.; O'Donnell, P.; Grigoriadis, A.; Diss, T.; Eskandarpour, M.; Presneau, N.; Hogendoorn, P. C.; Futreal, A.; Tirabosco, R.; Flanagan, A. M. IDH1 and IDH2 mutations are frequent events in central chondrosarcoma and central and periosteal chondromas but not in other mesenchymal tumours. *J. Pathol.* **2011**, *224*, 334−343.
(17) Sasaki, M.; Knobbe, C. B.; Munger, J. C.; Lind, E, F.; Brenner, D.; Brüstle, A.; Harris, I. S.; Holmes, R.; Wakeham, A.; Haight, J.; You-Ten, A.; Li, W. Y.; Schalm, S.; Su, S. M.; Virtanen, C.; Reifenberger, G.; Ohashi, P. S.; Barber, D. L.; Figueroa, M. E.; Melnick, A.; Zúñiga-Pflücker, J. C.; Mak, T. W. IDH1(R132H) mutation increases murine haematopoietic progenitors and alters epigenetics. *Nature* **2012**, *488*, 656−659.